Aqueous Ethylenediamine Dihydroxo Palladium(II): A Coordinating Agent for Low- and High-Molecular Weight Carbohydrates**

Reinhart Ahlrichs, Matthias Ballauff, Karin Eichkorn, Otto Hanemann, Gerhard Kettenbach, and Peter Klüfers*

Abstract: An aqueous solution of $[(en)Pd(OH)_2]$ (Pd-en) forms 1,2- and 1,3-diolato complexes on reaction with polyols. Three crystalline palladium(II) complexes have been isolated and characterized with anhydroerythritol (AnEryt), 1,6-anhydro-β-D-glucose (1,6AnGlc, levoglucosan), and sucrose (Suc) as the polyol components, namely $[(en)Pd(AnErytH_{-2})] \cdot 4H_2O$ **(1)**, $[(en)Pd(1,6AnGlc2,4H_{-2})] \cdot H_2O$ **(2)** and $[(en)_2Pd_2(Suc1,3,3',4'H_{-4})] \cdot 11H_2O$ **(3)**. Pd-en acts as a coordinating solvent for cellulose; the polysaccharide anhydro-glucose units (Glc$_C$) form $[(en)Pd(Glc_C2,3H_{-2})]$ entities on dissolution. The palladium-binding sites of the saccharides may be recognized by ^{13}C NMR spectroscopy in the case of 1,2-diolic chelator groups, which exhibit a downfield, coordination-induced shift of the two diolato carbon atoms of about 10 ppm. Slightly yellow, viscous solutions of cellulose in Pd-en, which are largely insensitive to oxidative degradation, were characterized by light scattering (LS). Analysis of the chain conformation by LS supports the significance of chain stiffening by intramolecular interresidue hydrogen bonds of the type O6′–H⋯O2⁻ in the molecularly dispersed and entirely metallated cellulose strands. The flexibility and energy of the hydrogen bond were investigated by density functional theory (DFT) calculations.

Keywords: carbohydrates · density functional calculations · NMR spectroscopy · palladium

Introduction

Carbohydrates are among the most abundant biogenic materials, cellulose being the most abundant of all, and are the objective of efforts aimed at increased use of renewable resources. Starch, sucrose and, with reservations, cellulose are available at prices comparable to those of synthetic organic base chemicals.[2] However, there are serious drawbacks to the development of carbohydrate-based chemistry, for example, the overfunctionalization of sucrose, which has eight non-equivalent hydroxyl groups. Strategies have been developed to overcome the high functionality by the well-established carbohydrate methodology,[3] whereas the more general route of reaction control with transition metal catalysis is largely underdeveloped in the carbohydrate field.[4] One of the most important reasons for the limited use of metal catalysis is the lack of knowledge of the bonding mode of carbohydrates towards transition metal ions. In the polysaccharide field, similar arguments hold with respect to the development of solvents of the Schweizer-reagent type,[5] which are capable of transforming cellulose, in particular, into a well-defined molecularly dispersed solution state, from which supramolecular polysaccharide-based aggregates may be built up.

Here we report that an aqueous solution of $[(en)Pd^{II}(OH)_2]$ (Pd-en) is a versatile agent for the analysis of carbohydrate–metal interactions in alkaline aqueous media. Structural principles of carbohydrate palladium complexes were derived from crystal structure data on $[(en)Pd(AnErytH_{-2})] \cdot 4H_2O$ **(1)**, $[(en)Pd(1,6AnGlc2,4H_{-2})] \cdot H_2O$ **(2)** and $[(en)_2Pd_2(Suc1,3,3',4'H_{-4})] \cdot 11H_2O$ **(3)**, and thus included both the 1,2- and 1,3-diolato coordination modes (AnEryt = anhydroerythritol; 1,6AnGlc = 1,6-anhydro-β-D-glucose (levoglu-

[*] Prof. Dr. P. Klüfers, Dipl.-Chem. G. Kettenbach
Institut für Anorganische Chemie der Universität
Engesserstrasse, Gebäude 30.45, D-76128 Karlsruhe (Germany)
Fax: (+49) 721-608-4290
E-mail: kluefers@achibm2.chemie.uni-karlsruhe.de
Prof. Dr. R. Ahlrichs, Dr. K. Eichkorn
Institut für Physikalische Chemie der Universität
Engesserstrasse, Gebäude 30.43, D-76128 Karlsruhe (Germany)
Prof. Dr. M. Ballauff, Dr. O. Hanemann
Polymer-Institut der Universität
Kaiserstrasse 12, D-76128 Karlsruhe (Germany)

cosan); Suc = sucrose, primed atoms: anhydroglucose residue; see Scheme 1). Studies of polysaccharide complexation by Pd-en focussed on cellulose. Light scattering and ^{13}C NMR spectroscopy on cellulose solutions support the structural model recently derived for the copper(II) – cellulose complex in Schweizer's reagent,[5] in which almost entirely metallated "ligand polymer" is formed in a "coordinating solvent". The limited flexibility of the metallated polysaccharide chain, which is a result of strong intramolecular, interresidue hydrogen bonding, was assessed by means of density functional theory (DFT) calculations.
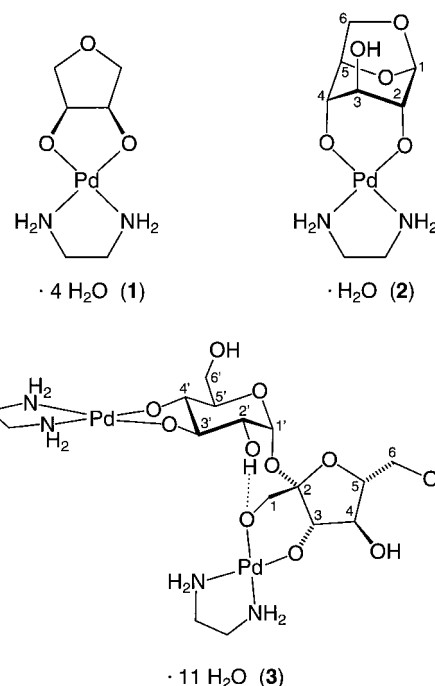
Experimental Section

[Pd(en)Cl₂] was prepared by Woernle's procedure:[6] PdCl₂ (532 mg, 3.00 mmol) was dissolved in hydrochloric acid (2 M, 4 mL) with gentle warming. The red solution was diluted with water to 15 mL. On dropwise addition of ethylenediamine (0.5 g) in water (5 mL) with stirring, a pink precipitate of [Pd(en)₂][PdCl₄] formed. After heating to 40–50 °C, addition of ethylenediamine solution was continued until the precipitate redissolved to give a pale yellow solution of [Pd(en)₂]Cl₂. The solution was filtered and acidified with hydrochloric acid (2 M) to precipitate [Pd(en)Cl₂] as small yellow needles. The mother liquor was cooled to about 4 °C for a few hours, and the precipitate was collected by filtration. Further product was collected by concentrating the filtrate and cooling again. Yield: 653 mg (92 %).

0.3 M Pd-en: [Pd(en)Cl₂] (499 mg, 2.10 mmol), silver(I) oxide (584 mg, 2.52 mmol) and water (7 mL) were stirred under nitrogen with exclusion of light at 50 °C. The solution was filtered, cooled (ice bath), and used immediately. Solutions of higher or lower concentration were prepared by varying the amount of water. The strongly alkaline Pd-en was kept under a nitrogen atmosphere to prevent absorption of carbon dioxide. All reactions with polyols were carried out with ice-bath cooling.

Ethylenediamine{*meso*-oxolane-3,4-diolato(2 −)}palladium(II) tetrahydrate (1): Anhydroerythritol (*meso*-oxolane-3,4-diol; 104 mg, 1.00 mmol) and Pd-en (0.2 M, 5 mL) were stirred for 1 h (ice bath, nitrogen atmosphere). The yellow solution was kept for 1 d at about 4 °C. After concentrating the solution to about 3 mL, acetone was added until weak

turbidity was visible. After filtration, diffusion of acetone/water (8/1) vapours at room temperature into the solution led to formation of yellow platelets.

Ethylenediamine{1,6-anhydro-*β*-D-glucos-2,4-ato(2 −)}palladium(II) monohydrate (2): 1,6-Anhydro-*β*-D-glucose (levoglucosan; 162 mg, 1.00 mmol) was used in the same way as described for **1**. Diffusion of acetone/water (4/1) vapours effected formation of yellow needles.

Bis(ethylenediamine){*μ*-*β*-D-fructofuranosyl-*O¹*,*O³*-*α*-D-glucopyranosid-*O³′*,*O⁴′*-ato(4 −)}dipalladium(II)} undecahydrate (3): Sucrose (205 mg, 0.6 mmol) and Pd-en (0.2 M, 6 mL) were stirred for 1 h (ice bath, nitrogen atmosphere). The yellow solution was kept for 2 d at about 4 °C. After concentrating the solution to about 4 mL, ethanol was added until weak turbidity was visible. After filtration, yellow needles of **3** formed at about 4 °C in the course of 2–3 d.

Solutions of cellulose in Pd-en: Cellulose samples and a slight excess (1.1 mol Pd per mole anhydroglucose) of Pd-en were stirred at 0 °C until dissolution of the polysaccharide was complete (ice bath; nitrogen atmosphere). Dissolution time depended on the degree of polymerization (DP) of the cellulose sample. Typical times were 1 d (Avicel, DP = 100), 3–4 d (pulp cellulose, nominal DP = 630), and 11–14 d (bleached cotton linters, nominal DP = 1100). If required, these solutions were diluted with aqueous sodium hydroxide.

^{13}C NMR spectra: About 100 mg of solid compound was dissolved in H₂O/D₂O (ca. 1.5 mL). Spectra of cellulose samples were recorded at 125.77 MHz (500 MHz spectrometer), and all others at 62.89 MHz (250 MHz spectrometer). Owing to the unexpected ^{13}C shifts of the levoglucosan compound (see Results and Discussion) the spectrum of **2** was assigned by 2D techniques, which were also applied to assign the superimposed signals of the fructose and glucose residues of **3**. Cellulose spectra were recorded on hydrolyzed regenerate cellulose (mean DP = 40). Spectra of the same material in Triton B (an aqueous solution of benzyltrimethylammonium hydroxide), aqueous sodium hydroxide and Cd-en[7] (Cadoxen) have been published recently.[29] Despite the low quality of these cellulose samples in terms of chemical uniformity and end-group content, advantage was taken of 1) their solubility in sodium hydroxide to provide a well-defined standard state, 2) the low viscosity of the samples and 3) their solubility in ethylenediamine-enriched Pd-en (Pd-2en), which allows the coordinating-solvent approach discussed to be investigated by ^{13}C NMR spectroscopy.

Scheme 1. Structurally characterized Pd-en complexes of anhydroerythritol (**1**), levoglucosan (**2**) and sucrose (**3**) anions.

Comment on German nomenclature: *Pd-en, eine wäßrige Lösung von [Pd(en)(OH)₂], ist ein* koordinierendes *Lösungsmittel für Cellulose und andere Polysaccharide, es löst Cellulose unter Bildung chelatisierender Diolato(2 −)-Komplexe mit nahezu jeder verfügbaren Diolfunktion. Das bekannteste koordinierende Lösungsmittel ist Schweizers Reagenz (Cu-NH₃, Cuoxam), in dem jedoch anders als in Pd-en wegen der Bildung auch homoleptischer Bis(diolato)-metallate Quervernetzung der Polymerketten zu beachten ist. Koordinierende Celluloselösungsmittel sind derzeit die einzigen nichtderivatisierenden Lösungsmittel, für die eine molekulardisperse Auflösung der Cellulose nachgewiesen ist. Im Deutschen wird die Bezeichnung* koordinierende Lösungsmittel *vorgeschlagen, um diese Solvenzien von den ebenfalls Metall-basierten, aber* nichtkoordinierenden *Lösungsmitteln wie Cd-en (Cadoxen) abzugrenzen. Der Begriff „komplexierendes" Lösungsmittel wird vermieden, da „Komplexbildung" im Kontext der Amylose-Einlagerungsverbindungen und der Wirt-Gast-Verbindungen mit Cyclodextrinen in der Kohlenhydratchemie auch für metallfreie Systeme verwendet wird.*

Crystallography: Crystal structure data of **1–3** are summarized in Table 1. Measurements were performed on a Stoe Stadi 4 four-circle diffractometer or a Stoe IPDS area detector (graphite monochromatized $Mo_{K\alpha}$ radiation). The programs used for structure solution, refinement, interpretation and graphical representation were SHELXS,[8] SHELXL,[9] ORTEP III,[10] PLATON95[11] and SCHAKAL,[12] respectively. Full-matrix refinement was performed on F^2, and the residuals are defined by $R(F) = \Sigma\Delta_1/\Sigma|F_o|$ with $\Delta_1 = ||F_o| - |F_c||$, $wR(F^2) = \{\Sigma(w\Delta_2^2)/\Sigma w(F_o^2)^2\}^{1/2}$ with $\Delta_2 = |F_o^2 - F_c^2|$, weights are defined by $w^{-1} = \sigma^2(F_o^2) + (xP)^2 + yP$; $3P = \max(F_o^2, 0) + 2F_c^2$. The goodness of fit is defined by $S = \{\Sigma(w\Delta_2^2/(N_{hkl} - N_{parameters})\}^{1/2}$, secondary extinction was corrected according to the SHELXL algorithm. Further details of the crystal structure investigations may be obtained from the Fachinformationszentrum Karlsruhe, D-76344 Eggenstein-Leopoldshafen, Germany (fax: (+49) 7247-808-666; e-mail: crysdata@fiz-karlsruhe.de), on quoting the depository numbers CSD-407 636 (**1**), CSD-407 637 (**2**) and CSD-407 635 (**3**). To allow convenient input of the crystallographic information file (CIF) of **3** into some computer programs, the numerical part of the atom labelling has been coded according to: n to $n1$ and n' to $n2$, e.g. O2 to O21 and C3' to C32, in the CIF.

Light scattering: Measurements were performed on a pulp cellulose termed Z630 (Buckey V68) and two samples of bleached cotton linters termed L800 and L1100 (Temming). All samples were thoroughly characterized by standard methods (viscosimetry in Cu-en and viscosimetry/GPC of tricarbanilates)[13] and by viscosimetry in Pd-en.[13] A 0.25 M solution of Pd-en was used for dissolving cellulose. Dilution was effected by adding 0.05 M aqueous NaOH with stirring and ultrasonification for 30 min. All alkaline solutions were protected from contact with air. Light-scattering intensities were recorded with a SOFICA-P6D42000 apparatus equipped with a laser (633 nm); all solutions were filtered through a hydrophilic filter (Gelman Science, nominal pore size 450 nm). The refractive index increment dn/dc

was determined with a Brice-Phoenix differential refractometer at two different wavelengths and extrapolated to 633 nm. The resulting increment of 0.182 mL g^{-1} was used in the subsequent analysis.

DFT Calculations: Calculations were performed within the framework of density functional theory[14] since this method has proved useful both in the treatment of transition metal compounds[15] and for describing hydrogen bonds.[16] The calculations were carried out with the program system TURBOMOLE[17] within the efficient RI-*J* approximation[18] with the Becke–Perdew (B–P) functional,[19] basis sets of SVP (split valence plus polarization)[20] and TZVP-type (triple zeta valence plus polarization)[21] and the corresponding auxiliary basis sets.[22] The abbreviation SVP/BP means that a basis set of SVP quality was employed within the DFT-BP approximation. Palladium atoms were treated by employing an effective core potential (ECP) which described the inner shells (28 core electrons) and included relativistic corrections.[23]

Results

Preparation of Pd-en/carbohydrate solutions: Pure Pd-en is a strongly alkaline solution which must be kept under nitrogen or argon to prevent carbon dioxide absorption. At room temperature, Pd-en slowly decomposes (a 0.5 M solution turns dark in the course of 1 d; more dilute solutions are more stable), but conducting all reactions in an ice bath sufficiently prevents precipitation of palladium metal. Addition of a carbohydrate enhances the redox stability. Although the

Table 1. Crystal structure data of **1–3**.

	1	**2**	**3**
formula	$C_6H_{14}N_2O_3Pd \cdot 4H_2O$	$C_8H_{16}N_2O_5Pd \cdot H_2O$	$C_{16}H_{34}N_4O_{11}Pd_2 \cdot 11H_2O$
M_r [g mol^{-1}]	340.67	344.66	869.47
water content [mass %]	21.2	5.2	22.8
crystal system; crystal class	monoclinic; 2-C_2	orthorhombic; 222-D_2	orthorhombic; 222-D_2
space group	$P2_1$	$P2_12_12_1$	$P2_12_12_1$
a [pm]	521.46(8)	772.70(10)	1302.0(3)
b [pm]	907.39(11)	1236.2(4)	1594.5(2)
c [pm]	1352.1(2)	1254.5(2)	1635.1(2)
β [°]	91.67(2)	90	90
V [10^6 pm^3]; Z	639.51(15); 2	1198.3(5); 4	3394.5(10); 4
calc. density [g cm^{-3}]	1.7692(4)	1.9105(8)	1.7014(5)
crystal size [mm]	$0.28 \times 0.18 \times 0.10$	$0.28 \times 0.10 \times 0.05$	$0.28 \times 0.15 \times 0.05$
T [K]	298	200	200
diffractometer	Stoe Stadi 4[a]	Stoe IPDS	Stoe IPDS
crystal-to-plate distance [mm]	–	60	70
ϕ range; ϕ increment [°]	–	1.8	1.0
exposure time per image [min]	–	12	16
refls. for unit cell det.	42	834	570
μ [mm^{-1}]	1.473	1.568	1.147
2θ range [°]	3–50	10–52	8.6–50
reflections collected	2137	5932	17724
unique reflections	1658	2222	5784
R_{int}; mean $\sigma(I)/I$	0.0275; 0.0241	0.0278; 0.0215	0.0512; 0.0371
observed refls., $I \geq 2\sigma(I)$	1613	2154	5369
parameters; restraints	183; 1	226	477; 38
$wR(F^2)$; $R(F)_{obs}$	0.0744; 0.0288	0.0523; 0.0206	0.0896; 0.0355
S; maximum shift/error	1.200; 0.001	1.043; 0.001	1.085; 0.002
treatment of H atoms	[b]	[c]	[d]
extinction coefficient	0.033(2)	–	–
$|\Delta\rho|$ [10^{-6} e pm^{-3}]	0.477	0.344	1.118
x, y (weighting scheme)	0.0310; 1.1471	0.0310; 1.0935	0.0398; 9.3995
absolute structure[e]	– 0.06(7)	– 0.05(3)	– 0.04(3)

[a] ω/θ scans, 4-32-4 steps for background-peak-background, minimum/maximum 0.5/2 s per step, three standard reflections every 3 h; empirical absorption correction, transmission factors from 0.6849 to 0.7827. [b] Common U_{iso} for all hydrogen atoms, H atoms bound to C geometrically fixed (C–H = 97 pm). [c] x, y, z, U_{iso} for all hydrogen atoms freely refined. [d] Common U_{iso} for H atoms bound to C and N, common U_{iso} for O-bound hydrogen atoms, O–H and H $\cdots$ H restrained to 83 and 131 pm, respectively, the latter to fix the H-O-H angle; [e] H. D. Flack, *Acta Crystallogr. Sect. A,* **1983**, *39*, 876–881.

strongly coordinating Pd-en dissolves cellulose samples of any degree of polymerization (DP) without activation, high-DP cellulose needs prolonged reaction times due to the slow kinetics of ligand substitution at the palladium centre. Typical periods of time until clear solutions are formed range from one day for Avicell samples (DP = 100) to 14 d for bleached cotton linters (DP = 1100). The maximum amount of cellulose dissolved in a given Pd-en quantity is in accord with 1:1 complexation, that is, each anhydroglucose monomer of the polysaccharide is bound to one palladium atom. Besides cellulose, amylose from starch, enzymatically synthesized amylose, and xylan from oat spelt are dissolved by Pd-en.

Crystal structures: Yellowish monoclinic crystals of $[(en)Pd(AnErytH_{-2})] \cdot 4 H_2O$ (**1**) were grown from solutions of Pd-en and anhydroerythritol (AnEryt; molar ratio Pd/ AnEryt = 1/1). In the crystal structure, a *meso*-oxolanediolato(2 −) group formed by double deprotonation of the diol acts as a chelate ligand in a heteroleptic, square-planar ethylenediamine – palladium(II) complex (Figure 1).
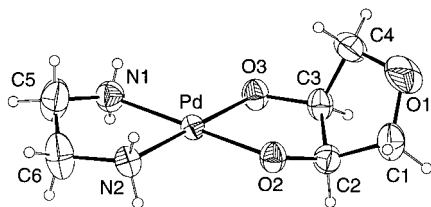

Figure 1. ORTEP plot of the structure of **1** (50 % probability ellipsoids). Selected distances [pm] and angles [°]: Pd – O2 198.8(5), Pd – O3 199.3(5), Pd – N2 203.3(6), Pd – N1 204.5(6), O1 – C1 141.7(10), O1 – C4 141.9(9), O2 – C2 142.5(8), O3 – C3 141.1(8), C1 – C2 151.7(10), C2 – C3 152.5(9), C3 – C4 151.7(10); O2-Pd-O3 85.5(2), N2-Pd-N1 83.8(3); O2-C2-C3-O3 − 38.7(8), N1-C5-C6-N2 47.6(12).

Owing to the sterical advantage of the furanoid $AnErytH_{-2}$ ligand,[24] the shortest Pd – O distances of this work were found for **1**. Though not forced by a chiral ligand, crystals of **1** belong to the noncentrosymmetric crystal class 2 (C_2) due to a polar arrangement of the complex molecules and the surrounding hydrogen-bonded water molecules.

Orthorhombic crystals of $[(en)Pd(Glc1,6An2,4H_{-2})] \cdot H_2O$ (**2**) were formed in an analogous reaction from Pd-en and 1,6-anhydro-β-D-glucose (Glc1,6An; levoglucosan). Levoglucosan can act as a 1,3-diolato ligand by bonding through O2 and O4. In fact, **2** is a six-membered ring chelate complex. From the crystal structure of levoglucosan itself, a diolato moiety with an unusually large bite of about 330 pm might be expected.[25] However, the molecular structure of **2** (Figure 2) again[26] shows flexibility of the bicyclic ligand, which undergoes distortion of the pyranose chair towards a boat conformation. In this distortion, greater flattening of the pyranose ring at C3 corresponds to an increasing O2 – O4 distance. Conversely, in **2** the respective hydroxyl groups occupy a more axial position, and the bite is smaller than in the free anhydro sugar. This can be compared with the even smaller O···O distance in $Li_2[Cu(Glc1,6An2,4H_{-2})_2] \cdot 4 H_2O$;[26] with the flexible levoglucosan ligand, adaption of
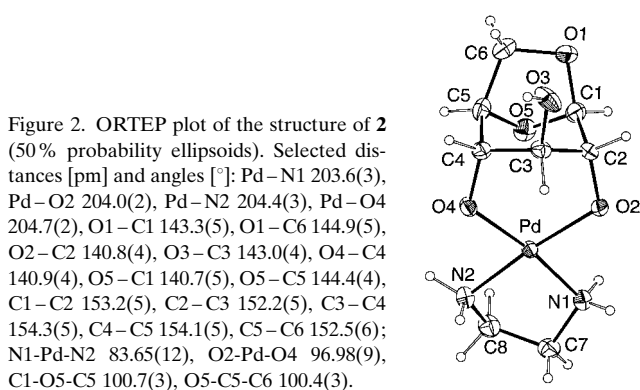

Figure 2. ORTEP plot of the structure of **2** (50 % probability ellipsoids). Selected distances [pm] and angles [°]: Pd – N1 203.6(3), Pd – O2 204.0(2), Pd – N2 204.4(3), Pd – O4 204.7(2), O1 – C1 143.3(5), O1 – C6 144.9(5), O2 – C2 140.8(4), O3 – C3 143.0(4), O4 – C4 140.9(4), O5 – C1 140.7(5), O5 – C5 144.4(4), C1 – C2 153.2(5), C2 – C3 152.5(5), C3 – C4 154.3(5), C4 – C5 154.1(5), C5 – C6 152.5(6); N1-Pd-N2 83.65(12), O2-Pd-O4 96.98(9), C1-O5-C5 100.7(3), O5-C5-C6 100.4(3).

the bite to the different radii of the metals, expressed in terms of the O···O distance, is twice that of simple 1,2-diols.

The lack of structural information on carbohydrate – metal complexes is exemplified by the fact that for sucrose, the most abundant nonpolymeric biogenic raw material, no structural data is available that reveal the metal binding sites of this economically important disaccharide. With Pd-en, yellow, orthorhombic crystals of the binuclear sucrose complex $[(en)_2Pd_2(Suc1,3,3',4'H_{-4}) \cdot 11 H_2O$ (**3**) were obtained from solutions of sucrose with a disaccharide/palladium molar ratio of 1/2. The structural analysis (Figure 3) revealed fourfold
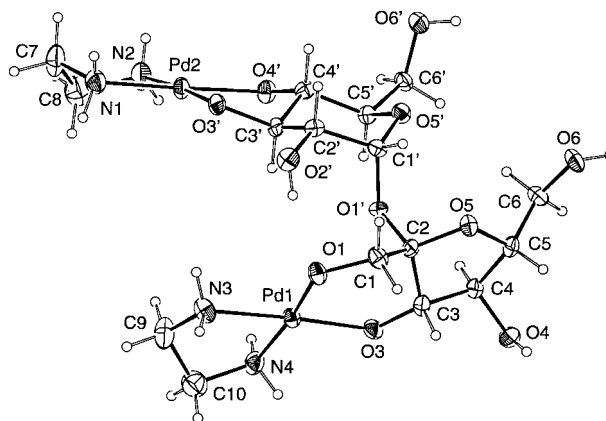

Figure 3. ORTEP plot of the structure of **3** (50 % probability ellipsoids). Selected distances [pm] and angles [°]: Pd1 – O3 201.7(4), Pd1 – N4 203.2(5), Pd1 – N3 203.2(5), Pd1 – O1 204.1(4), Pd2 – O3′ 201.2(4), Pd2 – O4′ 202.1(4), Pd2 – N1 203.6(5), Pd2 – N2 204.9(5), O1 – C1 142.2(6), O1′ – C2 143.0(6), O1′ – C1′ 143.2(6), O2′ – C2′ 141.6(6), O3 – C3 140.3(7), O3′ – C3′ 143.5(6), O4 – C4 141.9(7), O4′ – C4′ 142.8(7), O5 – C2 142.3(7), O5 – C5 146.3(7), O5′ – C1′ 141.2(7), O5′ – C5′ 144.4(6), O6 – C6 143.5(7), O6′ – C6′ 141.6(7), C1 – C2 150.3(8), C1′ – C2′ 152.1(8), C2 – C3 152.3(8), C2′ – C3′ 150.7(7), C3 – C4 152.4(8), C3′ – C4′ 152.1(7), C4 – C5 154.2(8), C4′ – C5′ 152.6(7), C5 – C6 149.6(8), C5′ – C6′ 152.1(8); N4-Pd1-N3 83.4(2), O3-Pd1-O1 98.62(15), O3′-Pd2-O4′ 86.18(15), N1-Pd2-N2 83.5(2); O2′-C2′-C3′-O3′ 55.3(6), O3′-C3′-C4′-O4′ − 57.0(6).

deprotonated sucrose ligands. The (en)Pd entities are attached to 1,2- and 1,3-diolate groups to form five- and six-membered chelate rings. In the anhydroglucose moiety, O3′ and O4′ act as ligators, while O1 and O3 are deprotonated and bound to palladium in the anhydrofructose part of the sucrose molecule. The *trans* geometry of the fructose 3,4-diol group is unsuitable for chelate formation. The conformation of the

disaccharide ligand is fixed by an intramolecular O2'-H···O1 bond.

Two typical features of the hydrogen bond patterns of **1–3** must be taken into account when constructing a bonding model of a polysaccharide in Pd-en. Firstly, two hydrogen bonds are directed towards each alkoxide group (Table 2); secondly, there is a pronounced tendency to form cooperative hydrogen-bond sequences. In crystals of **3**, all common structural elements of hydrogen-bond systems are present (Scheme 2): a four-membered homodromic ring (bottom right), a five-membered heterodromic cycle (top), and an infinite cooperative chain (see legend).[27]

The geometry at the acceptor oxygen atoms is almost tetrahedral, thus formally both lone pairs of the oxygen atoms are used. The significance of intramolecular hydrogen bonding is emphasized by the structure of **3**, which shows a conservative hydrogen-bond management in that the usual O2'···O1 bond of the uncomplexed sucrose molecule is left intact and is strengthened by deprotonation of the acceptor and by fixing the direction of the O–H vector.

^{13}C NMR spectroscopy: ^{13}C NMR spectra of **1** exhibit a downfield coordination-induced shift (CIS) of about $\Delta\delta =$ 10 ppm for the (equivalent) carbon atoms attached to the ligating oxygen atoms O2 and O3 relative to a solution of the

corresponding carbohydrate in an aqueous sodium hydroxide solution of the same hydroxide concentration. Coordination-induced shift is a well-known feature of the ^{13}C NMR spectra of polyolato complexes of molybdenum and tungsten.[28] In contrast, no CIS is observed for **2**; the ^{13}C NMR chemical shifts of C2 and C4 are essentially the same as those of free levoglucosan. The ^{13}C NMR spectrum of **3** is characteristic of 1,2- and 1,3-diolate complexation. The assignments given in Table 3 was established by 2D techniques, and ambiguity remained only for three signals in the narrow range of $\delta =$ 83.1–83.4 ppm. Spectra of sucrose/Pd-en solutions with molar ratios of 1/1 to 1/5 exhibit more signals, indicating the presence of more than one species at a given molar ratio.

In the yellow viscous solutions of cellulose in Pd-en, the anhydroglucose monomer units of the polysaccharide chains are entirely complexed according to ^{13}C NMR data (Table 3). The uniform chemical environment of all of the anhydroglucose units is shown by the sharp and unsplit main signals of the glucose carbon atoms in the ^{13}C NMR spectrum of a DP40 cellulose sample (Figure 4; the weaker signals are due to marked enrichment of DP40 cellulose with poorly defined end-groups). Moreover, the spectrum shows a CIS of 10 ppm for the C2 und C3 signals. Even the C1 signal, which sometimes splits into a doublet in cellulose solutions,[29] is a singlet in Pd-en. As a whole, the spectrum is in accord with the

Table 2. Hydrogen bonds in **1–3** (D = donor, A = acceptor, deprotonated acceptors underlined); distances [pm] and angles [°]; water-oxygen atoms are labelled O9...; alkoxo acceptors are underlined; symmetry codes apply to A and are of the form *n.uvw*; *n* = 1: *x*, *y*, *z*; codes with *n* > 1 are given at the compound numbers. Note the restraints in hydrogen atom refinement of **3** (Table 4).

D	H	A	D–H	H···A	D···A	D–H···A	*n.uvw*
1 (symmetry code: *n* = 2: −*x*, *y* + 1/2, −*z*):							
N1	H711	O94	84(10)	220(11)	301.7(9)	165(10)	2.655
N1	H712	O91	68(11)	234(11)	299.8(10)	162(12)	1.655
N2	H721	O92	85(10)	211(10)	295.6(9)	173(10)	1.655
N2	H722	O93	89(11)	229(11)	310.2(9)	151(9)	2.656
O91	H911	O3	81(11)	185(11)	266.7(8)	178(11)	
O91	H912	O94	74(12)	212(12)	282.9(10)	160(11)	2.655
O92	H921	O93	83(11)	204(12)	282.8(10)	159(10)	2.656
O92	H922	O2	61(11)	206(11)	266.4(7)	170(14)	
O93	H931	O92	80(11)	212(11)	287.3(9)	155(10)	1.655
O93	H932	O2	72(11)	205(11)	275.9(8)	169(12)	
O94	H941	O3	85(11)	186(10)	270.3(8)	173(10)	
O94	H942	O91	69(12)	216(12)	282.2(9)	161(12)	1.655
2 (symmetry codes: *n* = 3: −*x*, *y* + 1/2, −*z* + 1/2; *n* = 4: *x* + 1/2, −*y* + 1/2, −*z*):							
O3	H83	O91	77(5)	188(5)	262.6(4)	162(5)	3.655
N1	H711	O4	80(4)	221(4)	291.7(4)	148(4)	4.566
N1	H712	O3	85(6)	212(6)	293.8(5)	164(5)	3.645
N2	H721	O2	82(5)	198(5)	279.3(4)	175(4)	4.466
N2	H722	O91	97(6)	232(6)	313.4(5)	141(4)	1.455
O91	H911	O4	87(5)	176(5)	263.7(4)	179(5)	1.655
O91	H912	O2	81(5)	200(5)	276.1(4)	156(5)	
3 (O···O$_{Suc}$ bonds only; symmetry codes see **2**, in addition: *n* = 2: −*x* + 1/2, −*y*, *z* + 1/2;):							
O2'	H822	O1	83(6)	186(7)	265.7(6)	161(7)	
O4	H84	O97	83(4)	201(3)	282.8(7)	171(9)	
O6	H86	O3'	82(4)	183(5)	263.6(5)	168(9)	2.664
O6'	H862	O1	83(6)	182(6)	264.6(6)	175(9)	2.664
O91	H912	O3'	83(4)	193(3)	272.3(6)	160(7)	3.646
O93	H931	O2'	83(5)	195(5)	277.4(7)	168(7)	3.746
O94	H941	O4'	83(5)	188(5)	269.2(6)	168(8)	1.655
O95	H952	O6	83(6)	206(7)	285.8(6)	161(8)	3.746
O96	H961	O4	83(5)	201(4)	282.1(7)	166(8)	4.456
O96	H962	O4'	83(4)	184(4)	265.6(7)	169(9)	
O98	H982	O3	82(6)	186(6)	267.4(7)	170(9)	
O910	H903	O6'	83(3)	193(3)	276.1(8)	177(10)	2.665
O911	H914	O3	83(7)	204(7)	279.0(8)	150(6)	
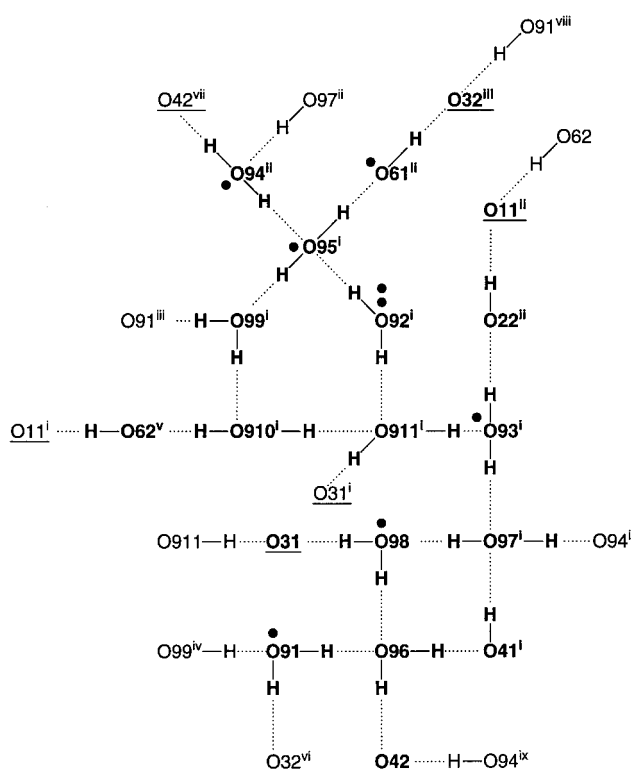
Scheme 2. Hydrogen bonds in **3**. Oxygen donors only; acceptors of an N-H···O bond are labelled by a bold dot; all hydrogen bonds are drawn for atoms in boldface; alkoxo acceptors are underlined. Symmetry codes in the form $n.uvw$ with $n = 1$: x, y, z; $n = 2$: $-x + 1/2, -y, z + 1/2$; $n = 3$: $-x, y + 1/2, -z + 1/2$; $n = 4$: $x + 1/2, -y + 1/2, -z$; translation $= u - 5, v - 5, w - 5$: [i] 4.456, [ii] 2.664, [iii] 1.554, [iv] 4.457, [v] 3.645, [vi] 3.646, [vii] 2.564, [viii] 3.655, [ix] 1.655. Note the infinite cooperative path: O97[ii] →O94[ii] →O95[i] →O99[i] → O910[i] →O911[i] →O93[i] →O97[i] →...

Table 3. ^{13}C NMR data for some of the compounds studied. First line: ^{13}C NMR shift in ppm; second line: shift with respect to free ligand in aqueous sodium hydroxide. Bold: carbon atoms attached to palladium-bound oxygen atoms; *italics*: carbon-2 atom in a 1,3-diolate; cellulose: degraded rayon (DP 40); mode: coordination of a 1,2- or a 1,3-diolate.

	C-1	C-2	C-3	C-4	C-5	C-6	Mode
1	73.2	**83.7**					1,2
	0.8	**10.4**					
2	102.3	**68.3**	*77.2*	**68.8**	77.3	64.7	1,3
	0.2	**− 2.5**	*4.4*	**− 2.7**	0.3	− 1.1	
3-Fru*f*	**65.1**	*108.6*	**83.1**	79.9	75.2	63.5	1,3
	2.2	*4.4*	**1.1**	2.9	0.6	1.6	
3-Glc*p*	92.9	75.5	**83.4**	**83.2**	74.4	61.0	1,2
	0.2	2.5	**10.3**	**13.4**	2.7	0.3	
Pd-en/cellulose	103.6	**84.5**	**84.5**	79.4	77.5	61.5	1,2
	− 0.9	**9.8**	**8.4**	0.4	− 0.8	0.0	
Pd-2en/cellulose	104.7	75.0	76.5	80.2	76.6	61.8	–
	0.2	0.3	0.4	0.4	0.3	0.3	

concept of molecularly dispersed single-stranded cellulose ligands in a strongly coordinating solvent.

The preference of palladium(II) centres for nitrogen instead of oxygen ligators is easily demonstrated by ^{13}C NMR spectroscopy. Addition of further ethylenediamine to Pd-en/ cellulose in an equimolar quantity with respect to palladium
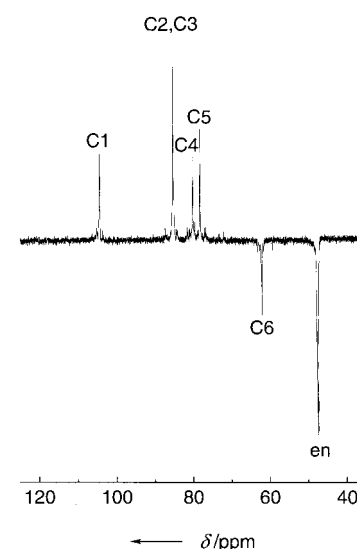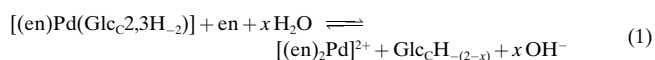

Figure 4. 125.77 MHz ^{13}C NMR DEPT spectrum of hydrolyzed regenerate cellulose (DP = 40) in Pd-en.

led to displacement of the diolato ligands according to Equation (1). The CIS vanished on addition of ethylenedi-

$$[(en)Pd(Glc_C2,3H_{-2})] + en + x\,H_2O \rightleftharpoons$$
$$[(en)_2Pd]^{2+} + Glc_CH_{-(2-x)} + x\,OH^- \quad (1)$$

amine, since the coordinating solvent Pd-en is converted into the noncoordinating solvent Pd-2en,[1b] which resembles simple alkaline media in its action on cellulose. When this experiment was conducted with cotton linters, addition of ethylenediamine caused precipitation of the polysaccharide; hence Pd-2en is a poorer solvent than Pd-en.

Viscosimetry and light scattering on Pd-en/cellulose solutions: Despite the well-known sensitivity to oxygen of cellulose solutions in copper-based solvents, especially Schweizer's reagent, the viscosity of Pd-en solutions is unaffected by oxidative degradation.[13] Light scattering (LS) experiments at 633 nm benefit from the yellowish colour of the palladium solvent, since there is no major absorption of light. The results of polymer characterization in Pd-en are listed in Table 4. The data given are in accord with the presence of molecularly dispersed and fully metallated cellulose strands, since P_n(Pd-en) is only slightly smaller than P_w(CTC)[13] (CTC = cellulose tricarbanilate), the more so since the difference is barely larger than the experimental uncertainty. Thus, like the ^{13}C NMR experiments, the LS data indicate uniform metallation of the repeating unit.

Table 4. Weight-average molecular weight M_w, radii of gyration $\langle s^2 \rangle_z^{1/2}$, number-average of degree of polymerization P_n, and persistence length l_p of cellulose samples as determined by light scattering in Pd-en.

Sample	M_w	$\langle s^2 \rangle_z^{1/2}$ [nm]	P_n[a]	l_p [nm]
Z630	176 000	39	539	9.6
L800	298 000	49	912	9.6
L1100	291 000	50	891	9.8

[a] Calculated as $M_w/326.65$, the denominator being the relative mass of an (en)Pd(Glc$_C$H$_{-2}$) repeating unit.

The radii of gyration $\langle s^2 \rangle_z$ obtained from light scattering were used together with the polydispersities[13] to calculate the persistence length l_p of the complexed cellulose chains. The theory of a wormlike chain according to Benoit and Doty[30] can be used to derive a relationship between the weight-average contour length L_w of monodisperse chains and l_p. Schmidt[31] has extended this theory to include nonuniform samples exhibiting a Schulz–Zimm distribution [Eq. (2)],
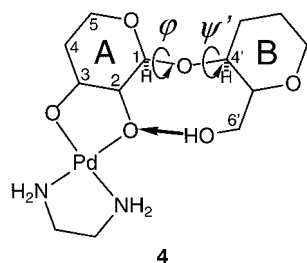
$$\langle s^2 \rangle_z = \frac{(m+2)l_p}{3y} - l_p^2 + \frac{2yl_p^3}{m+1} - \frac{2l_p^4}{m(m+1)}\left(y^2 - \frac{y^{m+2}}{(y+l_p^{-1})^m}\right) \qquad (2)$$

where $m = (M_w/M_n - 1)^{-1}$ and $y = (m+1)/L_w$. The values of l_p (Table 4) coincide for the three molecular weights investigated, indicating consistency of the data. The numerical value of the persistence length ($l_p = 9.6$ nm) corresponds to segments of about 20 anhydroglucose units and indicates stiffening of the cellulose chains upon complexation.

Although indicative of chain stiffening, the measured persistence length is considerably smaller than those of covalently substituted cellulose chains in the form of CTCs ($l_p = 17$ nm[32]). This finding is in accord with the structural model discussed below together with the flexiblity of the acetal links derived from the DFT calculations.

DFT calculations on a truncated cellobiosate(2 –) – Pd(en) complex: A metallated cellulose strand stiffened by intramolecular $O6'-H\cdots O2^-$ bonds is a ribbon of restricted flexibility. To obtain insight into the significance of the stiffening interresidue hydrogen bond $O6'-H\cdots O2^-$ in terms of geometry and energy, DFT calculations were performed on the truncated cellobiosate(2 –) – Pd(en) unit **4** (Scheme 3) of a palladium-coordinated cellulose chain. Initially the conformational energetics of the hydrogen-bond-supported acetal link of **4** were assessed at the SVP level, with the torsion angle $\psi' = $ C1-O1-C4'-C5' as the independent variable when forcing an entire turn of ring A relative to ring B (Figure 5). The energy profile shows a deep minimum for conformations that allow strong $O6'-H\cdots O2^-$ bonding to the deprotonated acceptor. Left of the minimum, the O6' hydroxymethyl group attached to ring B moves above ring A (Scheme 3) and the energy is high since O6'H forms bonds with the weaker acetal oxygen acceptors (O1, O5) and because the entire fragment has a less favourable conformation in terms of steric repulsion. The latter contribution is more pronounced to the right of the minimum, where the hydroxymethyl group moves below ring A and is heavily influenced by H1, which efficiently bars its path. Note the often irregular change in
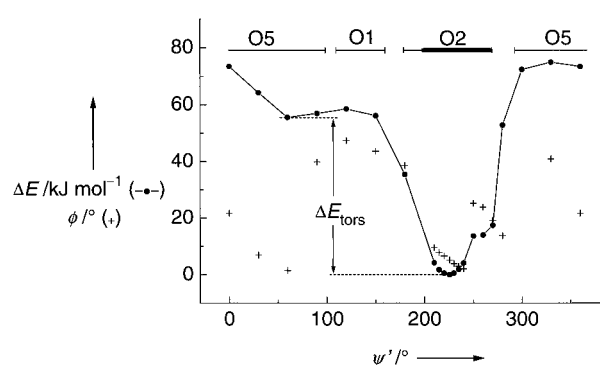
Scheme 3. The truncated Pd-en/cellobiosate(2 –) fragment used for DFT calculations. ϕ and ψ' are the torsion angles H1-C1-O1-C4' and C1-O1-C4'-C5', respectively; the latter has been introduced for technical reasons instead of the usual $\psi = \angle$ C1-O1-C4'-H4'.

Figure 5. Energy of the truncated cellobiose – Pd(en) entity of Scheme 3 at the SVP/BP level (minimum energy set to 0) versus ψ' (the C1-O1-C4'-O4' torsion angle); ϕ (the H1-C1-O1-C4' torsion angle) versus ψ'; not indicated in the diagram: $\phi(300°) = -161°$. The respective hydrogen bond acceptor of the pendant donor group O6'–H86' is indicated at the top of the diagram. A bold bar denotes strong hydrogen bonding (H$\cdots$acceptor distance < 160 pm). A hydrogen bond is present for each conformation except for that with $\psi' = 280°$. For definition of ΔE_{tors}, see text.

the relative orientation of the rings A and B depicted in Figure 5, as expressed by the torsion angle ϕ defined in Scheme 3. This is a result of allowing the structure to relax for each value of ψ', thus assuring smooth variation of energy at the expense of occasional abrupt changes in conformation along the torsional path. The repulsion term is least significant in the flat minimum at $\psi' = 60°$, where rings A and B are arranged almost coplanar in a rather unstrained conformation, as they are in the absolute minimum, but with rotation of one of the rings by about 180°.

The clearly resolved structure around the absolute minimum may be described in a simple electron-pair picture. Of the two lone pairs at O2, it is the equatorial pair (relative to the $^4C_1$ puckered ring A as a reference plane) that accepts the bond from the O6'H donor set in the minimum-energy structure. A slight increase in ψ' causes the donor to switch to the axial pair. This leads to the clearly resolved step on the right flank of the energy curve, which is about 13 kJ mol^{-1} less stable at the SVP level. The transition of the donor from one acceptor electron pair to the other evidently is a process with an activation barrier, since no intermediate geometry is tangible under the chosen restrictions of the refinement procedure. The abrupt change of conformation is directly shown in Figure 5 in the ϕ versus ψ' plot.

To assess a reasonable value for the energy content of the $O6'-H\cdots O2^-$ bond, the difference between the energies of the global and the flat minima ΔE_{tors} (Figure 5) was determined with the extended TZVP basis set to give 43 kJ mol^{-1} for the skip from the absolute minimum to the less favourable bonding situation in the flat minimum at $\psi' = 60°$ (cf. about 55 kJ mol^{-1} at the SVP level[33]). In the next step of the analysis, the Pd(en) entity of Scheme 3 was replaced by two hydrogen atoms to model the corresponding fragment of cellulose itself. The ΔE_{tors} value was now 11 kJ mol^{-1}, and the difference of 32 kJ mol^{-1} is the energy gain when the $O6'-H\cdots O2$ bond is strengthened by deprotonation of the acceptor. To assess the total energy of an $O6'-H\cdots O2^-$ bond, the energy of a normal $O-H\cdots OH$ hydrogen bond of about 22 kJ mol^{-1} has to be added,[34] and this gives a total of about 54 kJ mol^{-1}

for the stiffening bond of a metallated cellulose strand if this bond is the only hydrogen bond directed towards the O2⁻ acceptor.

An energy of 2.5 kJ mol⁻¹ ($= R \cdot 298$ K) for the minimum structure shows that the link is rather flexible. In terms of ψ', a 20° torsion may thus be expected at room temperature for each hydrogen-bond-supported acetal link.

Correspondence of geometrical data was improved by adding water donors to the alkoxo groups to model the typical environment of alkoxo double acceptors in crystal structures. Three water molecules were added to the diolato function of the minimum-energy structure to allow for hydrogen bonding, and the structure was optimized at the TZVP level. In the course of the refinement, the water molecules approached three of the nitrogen-bonded hydrogen atoms and established additional bonds. Though not in an environment typical for the crystal structures described here with respect to these additional intraresidue N–H···OH₂ bonds (which are established in an intermolecular mode in the crystalline state; see Scheme 2), the calculated structure more closely resembles the values found with the glucose moiety of **3**. To take hydrogen-bond cooperativity into account, a further water molecule was added to establish an HO–H···O6′–H···O2 chain. This resulted in only a slight change in geometry. Significant parameters illustrating the various levels of refinement are compiled in Table 5; the minimum-energy structure of the final refinement is depicted in Figure 6. Differences to

Figure 6. The minimum-energy structure of **4**·4H₂O. Selected distances [pm] and angles [°] (see also Tables 5 and 6): C1–C2 153.5, C2–C3 152.5, C3–C4 152.8, C4–C5 153.5, C1–O1 139.4, C1–O5 143.8, C2–O2 142.9, C3–O3 142.9, C5–O5 143.7, C4′–O1 143.8, C4′–C5′ 154.0, C5′–C6′ 153.7, C6′–O6′ 143.0; N1-Pd-N2 84.0, O2-Pd-O3 85.4, C1-O1-C4′ 118.7; O2-C2-C3-O3 57.8.

Table 5. Geometrical parameters as a function of model improvement, and corresponding distances [pm] in **3**.

	4	**4·3H₂O**	**4·4H₂O**	**3**
Pd–O2	199.3	201.7	205.3	202.1 (O4)
Pd–O3	201.8	205.9	205.1	201.2
Pd–N1	210.9	206.9	207.6	204.9 (N2)
Pd–N2	210.9	206.9	206.4	203.6 (N1)
O6′···O2	257.7	267.6	269.0	265.7 (O2′···O1)
$\psi^{min}/°$	224.6	219.8	219.8	

comparable crystal data are small, and, in the case of Pd–N and O···O distances, reflect the simplifications imposed on the level of approximation (note, in particular, the lengthening of the O6′–H···O2⁻ bond when additional donors to O2 are taken into account). Even the most polar Pd–O contacts match reliably.

Discussion

Palladium(II) is particularly suitable for the complexation of various types of diols. In this respect, it differs from iron(III) or the small beryllium ion, which exhibit a pronounced preference for furanoid diols (O-C-C-O: 0 to ca. 40°) over pyranoidic diols (O-C-C-O: 50 to 60°).[24b, c] Thus in **1** the ligand, though capable of adopting a small torsion angle when binding to small cations, exhibited rather large torsion of the diol group, which was also observed in the homologous bipyridyl complex.[35] In **2**, the bite of the flexible bicyclic
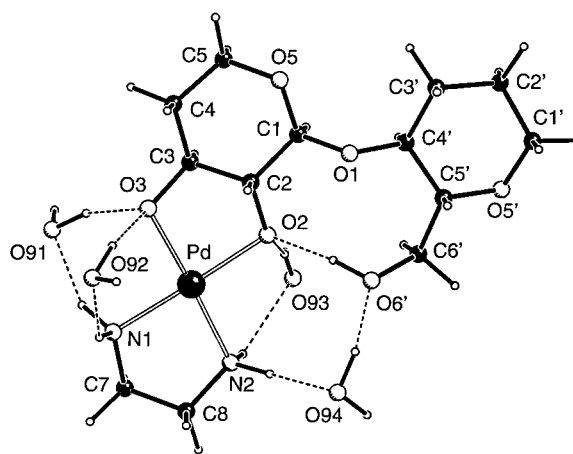
ligand is markedly larger than in a copper(II) levoglucosan complex.[26] Finally, in **3**, binding to a pyranoidic *trans*-diol in its equatorial/equatorial conformation takes place in the glucose part of the structure.

With Pd-en and sucrose, the pattern of metal-binding sites found in the crystalline state appears to be not the only one that is possible. Reaction mixtures with a palladium/sucrose ratio of 2/1 exhibit ¹³C NMR spectra with more signals than do re-dissolved crystals of **3**, even with samples that had long reaction times to take kinetic inertness into account. Accordingly, further reasonable dipalladium–sucrose complexes may exist, which appear to be roughly equivalent to **3** in terms of energy. Thus in a Fru*f*-O^4,O^6-Glc*p*-$O^{2'}$,$O^{3'}$ complex analogous diolate species are present, and even the intramolecular hydrogen bond may be formed although the O–H vector is reversed. The rather large number of signals at the high Pd/Suc ratio of 5/1 indicates that in addition to the Glc*p*-O^3,$O^{4'}$ the Fru*f*-O^1,O^3 and the Fru*f*-O^4,O^6 sites can not simultaneously act as ligands in a Pd₃-Suc species, as is shown by simple ball-and-stick models of the fructose part with an E_3 conformation. Since no other Pd₃–Suc species are expected for this stoichiometry when hydrogen bonding is taken into account, a maximum of only 12 signals should be obtained, but more are observed.

¹³C NMR spectra of **1** and of the glucose part of **3** exhibit deshielding of the alkoxo carbon atoms by about $\Delta\delta = 10$ ppm, which has also been observed for bis-ethylene-

Table 6. Hydrogen bonds in **4**·4H₂O (D = donor; A = acceptor; alkoxo acceptors are underlined); distances [pm] and angles [°].

D	H	A	D–H	H···A	D···A	D–H···A
O6′	H86′	O2	101.0	168.9	269.0	170.5
O91	H911	O2	99.6	181.1	277.1	160.8
O92	H921	O3	99.3	186.2	280.6	157.7
O93	H931	O3	100.8	170.9	268.7	162.2
O94	H941	O6′	100.9	166.2	266.0	169.1
N1	H711	O94	104.9	178.2	283.0	177.9

diamine-1,2-diolatocobalt(III) compounds[24a] and in sugar alcohol complexes of molybdenum and tungsten.[28] In contrast, the chemical shifts of **2** and of the fructose part of **3** seem to contradict the commonly accepted assumption that a carbohydrate carbon atom bearing a metal-bound oxygen atom can be recognized by a CIS of 10 ppm or more.[28] However, a CIS of 10 ppm at, for example, a d^0 molybdenum(VI) centre may be of different origin than the same shift caused by a low-spin d^8 palladium(II) center. Accordingly, the shifts reported here were not predicted exclusively from inductive effects.[36] The different CIS pattern of the 1,3-diolates also requires further investigation. NMR spectroscopy can be used as a diagnostic tool for examining carbohydrate complexation through 1,2-diol groups. Thus NMR spectroscopy on cellulose in Pd-en has provided the first evidence of metal coordination to the O2,O3 diol groups of the polysaccharide in the manner shown in Scheme 4. This is supported by an upfield shift of the C2
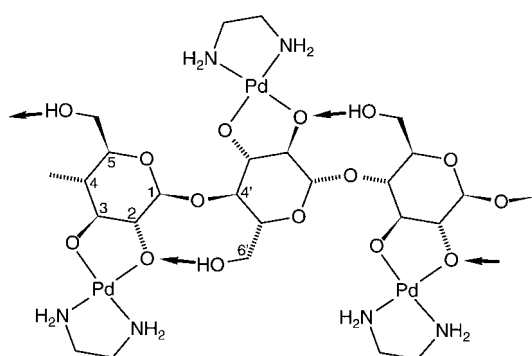
Scheme 4. Cellulose in Pd-en.

and C3 signals by $\Delta\delta = 10$ ppm on addition of ethylenediamine in equimolar amounts with respect to palladium, which cleaves the metal from the carbohydrate. The DP40 cellulose used in the NMR experiments remained dissolved in the alkaline solution of $[Pd(en)_2](OH)_2$ but now gave rise to a typical spectrum of cellulose in a noncoordinating metal-based solvent such as Cd-en (Table 3).[29]

The experiments on Pd-en thus give support to a new view of metal-based cellulose solvents, which is also supported by light-scattering experiments. Although apparently closely related, metal-based solvents be divided into two classes: Cd-en, Ni-en, Ni-NH$_3$ [1b] and other solvents with a high total concentration of dissolved metal hydroxide appear to be noncoordinating solvents which dissolve cellulose in the same way as aqueous alkylammonium hydroxide solutions, that is, by the action of high hydroxide concentration in the presence of a bulky cation that can support the separation of the cellulose chains. As with all other nonderivatizing cellulose solvents, the cellulose microfibrils are not disassembled to single cellulose chains in these solvents.[37]

In contrast, Schweizer's reagent (Cu-NH$_3$), Cu-en and the new solvents Pd-en, Ni-tren,[1a] Zn-dien and Cd-tren[38] are coordinating agents. They dissolve even an equimolar amount of cellulose monomer units at lower total metal hydroxide concentration to yield entirely metallated polysaccharide strands. A ligand polymer is formed, that is, a metal-containing polymer in which the ligand is the polymeric entity (cf. metal-containing polymers of the coordination polymer type). Coordinating agents are unique among the nonderivatizing solvents in forming single-stranded cellulose chains during the dissolution process. Concurrent with O2,O3 deprotonation, the deprotonated sites are fixed and at the same time are shielded from interchain hydrogen bonding. Thus, separation of the polysaccharide chains is achieved by the action of a suitable metal centre/auxiliary ligand combination. Due to tight metal-bonding to a well-defined site of the polysaccharide, the mere bulk of the metal/ligand moiety is less significant.

The question arises whether a coordinating solvent is still nonderivatizing. With Schweizer's reagent, the question may be answered in terms of kinetic lability. The constitution of the copper(II) cellulose complex varies apparently without delay in time when changing the solution composition in terms of pH or total concentration of the components. On the other hand, the Pd-en/cellulose complex appears to remain unaltered by these parameters for two reasons. Firstly, palladium(II) compounds are kinetically more inert than the highly labile copper(II) complexes; secondly, at an en/Pd/diol ratio of 1/1/1, no other stable species were detected even when the pH was increased, which favours bis-diolato-metallates in the cupric system (in the presence of nitrogen ligands, an O$_4$ ligator set is suitable for copper(II) but not for palladium ions).

The use of new coordinating solvents such as Pd-en, Ni-tren, Zn-dien and Cd-tren thus appears to be the key to manipulating single strands of underivatized cellulose. Hence, a suitable tool for the synthesis of supramolecular assemblies with cellulose and other polysaccharides is available. Pd-en is less suitable for synthetic purposes due to its high price and thermal instability, but it is well suited to the analysis of solutions of polysaccharides in coordinating solvents owing to its applicability in NMR spectroscopy and light scattering.

Conclusions

In the presence of carbohydrate-based 1,2- and 1,3-diol groups, the hydroxo ligands of Pd-en, an aqueous solution of $[(en)Pd(OH)_2]$, are replaced by a dianionic diolato(2–) ligand. The ligating alkoxo O atoms are acceptors in hydrogen bonds, which are established as intramolecular bonds whenever possible. Pd-en is a coordinating solvent for polysaccharides, including cellulose, which is molecularly dispersed to give entirely metallated single strands. A structural model of the metallated cellulose chains that are stiffened by intrachain interresidue hydrogen bonds with O6–H donor groups and O2′ alkoxo acceptors, in which the latter are part of chelate rings and hence have geometrically fixed lone pairs, is supported by a combined experimental and theoretical approach with 1) crystal structure analysis on low-molecular weight carbohydrates, 2) ^{13}C NMR spectroscopy on hydrolyzed cellulose samples (DP = 40), 3) light-scattering investigations on cellulose samples of various degrees of polymerization and 4) density functional theory calculations on a truncated Pd(en)–cellobiosate entity.

[1] a) J. Burger, G. Kettenbach, P. Klüfers, *Macromol. Symp.* **1995**, *99*, 113–126; b) *ibid.* **1997**, *120*, 291–301.

[2] F. W. Lichtenthaler, A. Boettcher in *Nachwachsende Rohstoffe—Perspektiven für die Chemie* (Ed.: G. Descotes), VCH, Weinheim, **1993**, pp. 151–168.

[3] M. Kunz in *Nachwachsende Rohstoffe—Perspektiven für die Chemie* (Ed.: G. Descotes), VCH, Weinheim, **1993**, p. 169–181; R. Schmidt, *ibid.*, p. 225–247; G. Wulff, *ibid.*, 281–300.

[4] For an early attempt with sucrose, see E. Avela, S. Aspelund, B. Holmbom, B. Melander in *Sucrochemistry (ACS Symp. Ser. 41)* (Ed.: J. L. Hickson), ACS, Washington, **1977**, pp. 62–76.

[5] W. Burchard, N. Habermann, P. Klüfers, B. Seger, U. Wilhelm, *Angew. Chem.* **1994**, *106*, 936–939; *Angew. Chem. Int. Ed. Engl.* **1994**, *33*, 884–887.

[6] M. Woernle, *Sitzungsber. phys.-med. Soz. Erlangen* **1906**, *38*, 285.

[7] Metal-based solvents are labelled following the scheme M-(*n*)L (M = metal, *n* = stoichiometric coefficient only if needed for discrimination, L = IUPAC-recommended abbreviation of the ligand). The nomenclature is illustrated in ref. [1b], and the known solvents are compiled.

[8] G. M. Sheldrick, SHELXS86, University of Göttingen, Germany, **1986**.

[9] G. M. Sheldrick, SHELXL93, University of Göttingen, **1993**.

[10] M. N. Burnett, C. K. Johnson, ORTEP-III. Report ORNL-6895. Oak Ridge National Laboratory, Tennessee, USA, **1996**.

[11] A. L. Spek, PLATON, *Acta Crystallogr. Sect. A*, 1990, *46*, C34; 1995 version.

[12] E. Keller, SCHAKAL, University of Freiburg (Breisgau), Germany, **1995**.

[13] O. Hanemann, M. Ballauff, *Macromolecules*, **1997**, *30*, 7638–7640.

[14] R. G. Parr, W. Yang, *Density-Functional Theory of Atoms and Molecules*, Oxford University Press, Oxford, **1989.**

[15] T. Ziegler, *Chem. Rev.* **1991**, *91*, 651–667.

[16] R. Kaschner, G. Seifert, *Int. J. Quantum Chem.* **1994**, *52*, 957–961.

[17] O. Treutler, R. Ahlrichs, *J. Chem. Phys.* **1995**, *102*, 346–354.

[18] K. Eichkorn, O. Treutler, H. Öhm, M. Häser, R. Ahlrichs, *Chem. Phys. Lett.* **1995**, *242*, 652–660.

[19] a) A. D. Becke, *Phys. Rev. A* **1988**, *38*, 3098–3100; b) S. H. Vosko, L. Wilk, M. Nusair, *Can. J. Phys.* **1980**, *58*, 1200–1211; c) J. P. Perdew, *Phys. Rev. B* **1986**, *33*, 8822–8824.

[20] A. Schäfer, H. Horn, R. Ahlrichs, *J. Chem. Phys.* **1992**, *97*, 2571–2577.

[21] A. Schäfer, C. Huber, R. Ahlrichs, *J. Chem. Phys.* **1994**, *100*, 5829–5835.

[22] K. Eichkorn, F. Weigend, O. Treutler, R. Ahlrichs, *Theor. Chim. Acta*, **1997**, *97*, 119–124.

[23] D. Andrae, U. Häussermann, M. Dolg, H. Preuss, *Theor. Chim. Acta* **1990**, *77*, 123–141.

[24] a) J. Burger, P. Klüfers, *Chem. Ber.* **1995**, *128*, 75–79; b) *Z. Anorg. Allg. Chem.* **1996**, *622*, 1740–1748; c) P. Klüfers, P. Mayer, J. Schuhmacher, *ibid.* **1995**, *621*, 1372–1378.

[25] Y. J. Park, H. S. Kim, G. A. Jeffrey, *Acta Crystallogr. Sect. B*, **1971**, *27*, 220–227.

[26] C. Gack, P. Klüfers, *Acta Crystallogr. Sect. C*, **1996**, *52*, 2972–2975.

[27] For definitions of terms concerning hydrogen bonds, see G. A. Jeffrey, W. Saenger, *Hydrogen Bonding in Biological Structures*, Springer, Berlin, **1991**.

[28] S. Chapelle, J.-P. Sauvage, J.-F. Verchère, *Inorg. Chem.* **1994**, *33*, 1966–1971; S. Chapelle, J.-P. Sauvage, P. Köll, J.-F. Verchère, *Inorg. Chem.* **1995**, *34*, 918–923.

[29] I. Nehls, W. Wagenknecht, B. Philipp, D. Stscherbina, *Prog. Polym. Sci.* **1994**, *19*, 29–78.

[30] H. Benoit, P. Doty, *J. Phys. Chem.* **1953**, *57*, 958–963.

[31] M. Schmidt, *Macromolecules* **1984**, *17*, 553–560.

[32] F. Fried, G. M. Searby, M. J. Seurin-Velluti, S. Dayan, P. Sixou, *Polymer* **1982**, *23*, 1755–1758; compare the persistence length of 13–22 nm of the highly stiffened poly-*p*-phenylenes: U. Tiesler, M. Rehahn, M. Ballauff, G. Petekidis, D. Vlassopoulos, G. Maret, H. Kramer, *Macromolecules* **1996**, *29*, 6832–6836; G. Petekidis, D. Vlassopoulos, P. Galda, M. Rehahn, M. Ballauff, *ibid.* **1996**, *29*, 8948–8953.

[33] The trend observed in the computed energy differences between the smaller (SVP) and the larger (TZVP) basis set is as expected: larger basis sets typically lead to relatively lower energies for strained systems and hydrogen bonds. Both effects tend to reduce the energy differences. We expect the error of the TZVP results to be smaller than the deviation between SVP and TZVP.

[34] R. Kaschner, G. Seifert, *Int. J. Quantum Chem.* **1994**, *52*, 957–961.

[35] M. Achternbosch, P. Klüfers, *Acta Crystallogr. Sect. C* **1994**, *50*, 175–178.

[36] U. Sternberg (Jena, Germany), private communication. Compare a CIS of only 5 ppm for tetracoordinate bis(diolato)antimonates(III): P. Klüfers, P. Mayer, *Z. Anorg. Allg. Chem.* **1997**, *623*, 1496–1498, which also points to the significance of the partly filled 3d shell of palladium(II).

[37] W. Burchard, private communication.

[38] P. Klüfers, P. Mayer, unpublished results.